Journal of Medicinal Chemistry

Article

pubs.acs.org/jmc

New Serotonin 5-HT$_{1A}$ Receptor Agonists Endowed with Antinociceptive Activity *in Vivo*

Margarita Valhondo,[†,∥] Isabel Marco,[†,⊥] Mar Martín-Fontecha,[†] Henar Vázquez-Villa,[†] José A. Ramos,[‡] Reinhard Berkels,[§] Thomas Lauterbach,[§] Bellinda Benhamú,*[,†] and María L. López-Rodríguez*[,†]

[†]Departamento de Química Orgánica I, Facultad de Ciencias Químicas, Universidad Complutense de Madrid, E-28040 Madrid, Spain

[‡]Departamento de Bioquímica y Biología Molecular, Facultad de Medicina, Universidad Complutense de Madrid, E-28040 Madrid, Spain

[§]UCB Pharma GmbH, Alfred-Nobel-Strasse 10, 40789 Monheim, Germany

Supporting Information

ABSTRACT: We report the synthesis of new compounds **4**−**35** based on two different openings (A and B) of the chromane ring present in the previously identified 5-HT$_{1A}$ receptor (5-HT$_{1A}$R) ligand **3**. The synthesized compounds were assessed for binding affinity, selectivity, and functional activity at the 5-HT$_{1A}$R. Selected candidates resulting from B opening were also evaluated for their potential antinociceptive effect *in vivo* and pharmacokinetic properties *in vitro*. Analogue **19** [2-(4-{[2-(2-ethoxyphenoxy)-ethyl]amino}butyl)tetrahydro-1*H*-pyrrolo[1,2-*c*]imidazole-1,3(2*H*)-dione] has been characterized as a high-affinity and potent 5-HT$_{1A}$R agonist (K_i = 2.3 nM; EC_{50} = 19 nM). Pharmacokinetic studies indicated that compound **19** displays a good metabolic stability in human liver microsomes ($t_{1/2}$ ∼ 3 h and CL_{int} = 3.5 mL/min/kg, at 5 μM), and a low level of protein binding (25%, at 5 μM). Interestingly, **19** (3 mg/kg, ip, and 30 mg/kg, po) caused significant attenuation of formalin-induced behavior in early and late phases of the mouse intradermal formalin test of pain, and this *in vivo* effect was reversed by the selective 5-HT$_{1A}$R antagonist WAY-100635. Thus, the new 5-HT$_{1A}$R agonist identified in this work, **19**, exhibits oral analgesic activity, and the results herein represent a step toward identifying new therapeutics for the control of pain.

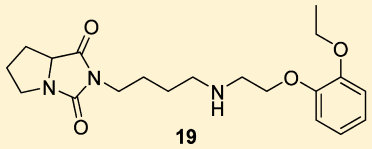

K_i = 2.3 nM
EC_{50} = 19 nM
efficacy in formalin test at 3 mg/kg, ip and 30 mg/kg, po

INTRODUCTION

Serotonin (5-hydroxytryptamine, 5-HT) mediates a plethora of physiological effects through at least 14 receptor subtypes, all but one belonging to the G-protein-coupled receptor (GPCR) or seven-transmembrane-spanning (7TM) receptor family. Defined on the basis of molecular, pharmacological, and functional criteria, 5-HT receptors have been classified into seven discrete subfamilies (5-HT$_1$ to 5-HT$_7$),[1] and their study for almost three decades has provided researchers with many targets for drug action. The 5-HT$_{1A}$ receptor (5-HT$_{1A}$R) was the first 5-HT subtype to be fully sequenced,[2] and it has also been the most extensively studied among serotonin receptors. Indeed, a large number of selective or multitarget 5-HT$_{1A}$R ligands have been developed so far with the aim of identifying new drugs, and this receptor still represents an attractive target for drug discovery.[3−7] In particular, 5-HT$_{1A}$R agonists and partial agonists have long shown to be clinically effective in the treatment of anxiety, depression, and psychosis.[8−15] More recently, the neuroprotective properties observed for some 5-HT$_{1A}$R agonists have suggested their utility for the treatment of ischemic stroke,[5,16−22] and these agents have also been proposed as levodopa adjuvants in the alleviation of dyskinesia in Parkinson's disease.[23,24] Moreover, one of the most attractive therapeutic potentials that has recently emerged for 5-HT$_{1A}$R agonists is that they may rival the opioids in pain relief therapy.[25] It is known that in nociceptive systems any input causes two effects that are opposite in sign. Activation of opioid receptors produces analgesia as a "first-order" effect and hyperalgesia as a "second-order" effect. The chronic treatment with opiods attenuates the first-order analgesia and strengthens the second-order hyperalgesia. According to this concept, it has been proposed that 5-HT$_{1A}$R activation has two effects that are opposite from those produced by opioids: pain as a first-order effect but also hypoalgesia as a second-order effect; with chronicity, this second-order hypoalgesia counteracts the first-order pain and remarkably develops into increasingly powerful analgesia.[26] This suggests that whereas repeated morphine administration leads to a loss of analgesic activity (tolerance) and even to hyperalgesia, repeated administration of a 5-HT$_{1A}$R agonist could produce the opposite effect, i.e., a progressive loss of acute hyperalgesia and an increase in analgesia.[27] These considerations stimulated pharmaceutical drug discovery that aimed to identify 5-HT$_{1A}$R agonists with high selectivity. In particular, the potent and selective 5-HT$_{1A}$R agonist F-13640 [befiradol, **1** (Chart 1)] demonstrated analgesic activity in animal models of acute and chronic pain comparable to those of large doses of opioid painkillers, but with fewer and less prominent side effects, as well as little or no development of tolerance with repeated use.[27,28] These studies represented a proof of concept that the 5-HT$_{1A}$R is involved in the regulation of nociceptive

Received: May 23, 2013
Published: September 19, 2013

   dx.doi.org/10.1021/jm400766k | *J. Med. Chem.* 2013, 56, 7851−7861

Chart 1. Structures of 5-HT$_{1A}$R Agonists Endowed with Antinociceptive Activity

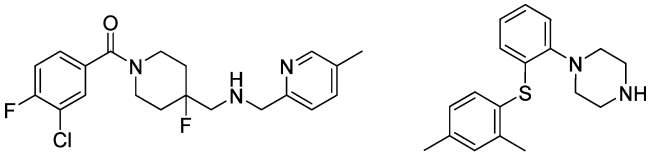

transmission. Therefore, 5-HT$_{1A}$R activation was proposed as a new molecular approach to the treatment of acute and chronic, nociceptive and neuropathic pain states. Indeed, the concept has been extended to other 5-HT$_{1A}$R agonists such as Lu AA21004 [vortioxetine, **2** (Chart 1)] that has shown analgesic activity in the formalin test.[29,30] Given the complexity of the mechanisms involved in pain modulation, it is not surprising that the application of single analgesic agents is not always effective in diverse painful conditions such as chronic pain syndromes. Thus, it is becoming clear that the combination of different mechanisms, which improves efficacy with reduced toxicity, is necessary for the reliable pharmacotherapy of pain. At present, there is evidence that the 5-HT$_{1A}$R may be used as a target in the search for new pharmacological approaches in the augmentation of analgesia. The ongoing clinical trials with compound **1**[31] have certainly reinforced the interest of 5-HT$_{1A}$R activation for the treatment of pain conditions. In this context, our goal is the development of a 5-HT$_{1A}$R agonist as an antinociceptive agent.

Over the past several years, our efforts in the search for new and selective 5-HT$_{1A}$R ligands have led to the discovery of several arylpiperazine-based 5-HT$_{1A}$R agonists endowed with anxiolytic properties.[3,32−37] More recently, we have developed new non-piperazine derivatives as second-generation 5-HT$_{1A}$R agonists exhibiting a neuroprotective effect against ischemic cell damage.[22,38] In these series, the modification of the different structural moieties of the molecule led to highest-affinity ligand **3** (Chart 2), which was characterized as a potent 5-HT$_{1A}$R agonist

Chart 2. Designed Compounds Based on A (4−7) or B (8−35) Opening of the Chromane Ring Present in the Previously Identified High-Affinity 5-HT$_{1A}$R Ligand 3

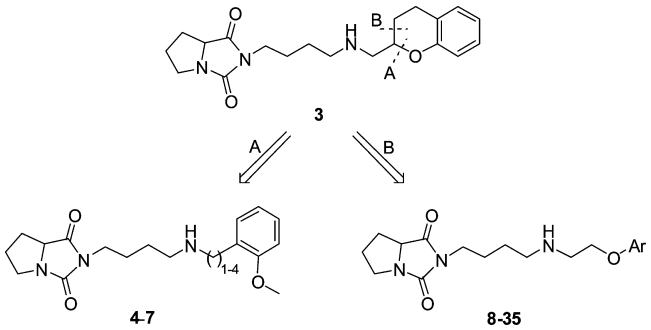

(K_i = 1.23 nM; EC_{50} = 16.3 nM). In this work, we aimed to generate structural variants of ligand **3**, focusing our attention on mimicking the chroman-2-ylmethyl group. In the new compounds, two different openings (A and B) of the chromane ring were considered (Chart 2). The synthesized compounds have been assessed for binding affinity, selectivity, and functional activity at the 5-HT$_{1A}$R. Selected candidates have also been evaluated for their potential antinociceptive effect *in vivo* and pharmacokinetic properties *in vitro*. In particular, compound **19** was characterized as a high-affinity and potent 5-HT$_{1A}$R agonist that exhibited oral analgesic activity in the mouse intradermal formalin test and a good pharmacokinetic profile.[39]

RESULTS AND DISCUSSION

Synthesis. Target compounds **4**−**7** based on A opening of the chromane ring in ligand **3** (Chart 2) were obtained by nucleophilic substitution of 2-(4-bromobutyl)tetrahydro-1*H*-pyrrolo[1,2-*c*]imidazole-1,3(2*H*)-dione (**36**) with the appropriate commercial *ω*-(*o*-methoxyphenyl)alkylamines or amine **37** in acetonitrile, which was prepared starting from 3-(2-methoxyphenyl)propanoic acid (Scheme 1). Final compounds **8**−**35** resulting from B opening of the chromane ring in ligand **3** (Chart 2) were synthesized starting from halogenated intermediate **36**, by reaction with appropriate 2-aryloxyethylamines **38**, or by alkylation of 2-(4-aminobutyl)tetrahydro-1*H*-pyrrolo[1,2-*c*]imidazole-1,3(2*H*)-dione (**39**) with corresponding 2-aryloxyethyl bromides **40**, as described in Scheme 2. Starting compound **39** was obtained by *N*-alkylation of hydantoin **41** with 4-chlorobutanonitrile in the presence of sodium hydride, followed by catalytic hydrogenation of intermediate **42**. Williamson reaction of appropriate phenols with 1,2-dibromoethane or 2-chloroacetamide in the presence of potassium carbonate and catalytic potassium iodide in refluxing 2-butanone afforded 2-aryloxyethyl bromides **40a**−**t** or intermediate 2-aryloxyacetamides **43a**−**g**. Subsequent reduction of **43a**−**g** with the borane dimethyl sulfide complex in diglyme yielded 2-aryloxyethylamines **38a**−**g**. Intermediate amine **38h** was prepared by Mitsunobu reaction starting from 8-hydroxyquinoline and *N*-(2-hydroxyethyl)phthalimide, followed by phthalimide cleavage.

Binding Affinities. New synthesized compounds **4**−**35** were converted to hydrochloride salts, and their affinities were evaluated at the 5-HT$_{1A}$R by radioligand binding assays (see the Supporting Information for details). High-affinity 5-HT$_{1A}$R ligands (K_i < 50 nM) were also assayed for selectivity over serotonin 5-HT$_{2A}$, 5-HT$_3$, 5-HT$_4$, and 5-HT$_7$ receptors.

Tables 1 and 2 show the calculated inhibition constants (K_i)[40] for target compounds **4**−**35** obtained from A and B openings of the chromane ring in ligand **3** (Chart 2). Clearly, A opening of chromane ring leads to a marked decrease or loss of affinity for the 5-HT$_{1A}$R, affording inactive or poorly active derivatives [K_i(**4**−**7**) ≥ 74 nM vs K_i(**3**) = 1.23 nM] (Table 1). On the other hand, compound **9** that results from B opening of chromane ring in compound **3** maintained a high affinity for the receptor [K_i(**9**) = 16.8 nM] (Table 1). Therefore, we decided to study the influence of several substituents at different positions of the aromatic ring in compounds **8** and **10**−**35**. From data in Table 1, in general ortho and meta positions are more favorable for 5-HT$_{1A}$R affinity than the para position, regardless of the nature of the substituent. Thus, all para-substituted derivatives are inactive, including those with substituents that provide high 5-HT$_{1A}$R affinity [K_i(**9**) = 16.8 nM and K_i(**10**) = 30 nM vs K_i(**11**) = 742 nM; K_i(**16**) = 4.8 nM and K_i(**17**) = 34 nM vs K_i(**18**) > 1000 nM]. Also, the presence of a substituent in the ortho position is in general more favorable than that in the meta position (see, for example, compounds **9** vs **10**, **13** vs **14**, and **16** vs **17**). Electron-withdrawing substituents seem to be detrimental for affinity even in the preferred ortho position [K_i(**24**) > 1000 nM and K_i(**27**) = 510 nM]. Accordingly, compounds bearing ortho-alkoxy groups displayed the highest 5-HT$_{1A}$R affinities [K_i(**16**) = 4.8 nM, and K_i(**19**) = 2.3 nM]. With regard to selectivity, in general, the new

dx.doi.org/10.1021/jm400766k | J. Med. Chem. 2013, 56, 7851−7861

Scheme 1. Synthesis of Target Compounds 4−7[a]

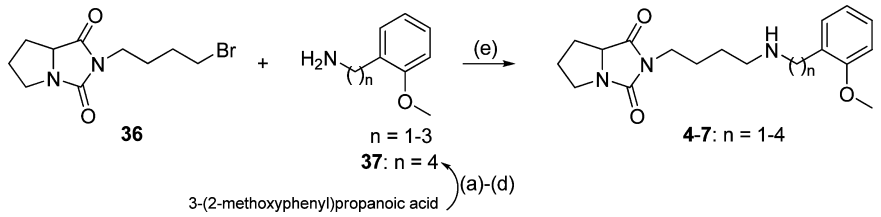

[a]Reagents and conditions: (a) $LiAlH_4$, Et_2O, rt, 20 h, 48%; (b) $SOCl_2$, toluene, pyridine, rt, 24 h, 77%; (c) KCN, KI, DMSO, rt, 3 h, 70%; (d) $LiAlH_4$, THF, rt, 3.5 h, 56%; (e) CH_3CN, 60 °C, 15 h, 30−52%.

Scheme 2. Synthesis of Target Compounds 8−35[a]

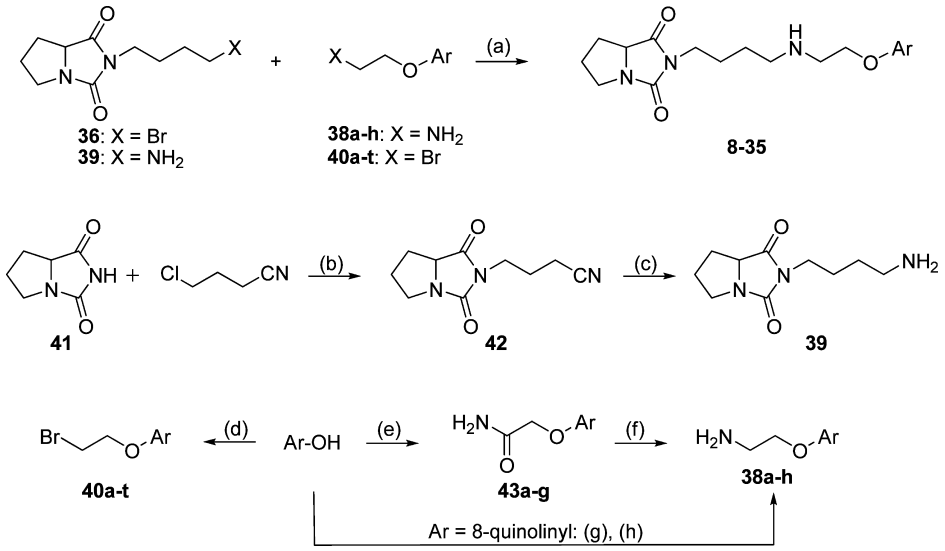

[a]Reagents and conditions: (a) CH_3CN, 60 °C, 15 h, 21−69%; (b) NaH, DMF, 110 °C, 4 h, 85%; (c) H_2, PtO_2, EtOH, rt, 15 h, 35%; (d) $Br(CH_2)_2Br$, K_2CO_3, KI, 2-butanone, Δ, 48 h, 30−67%; (e) $ClCH_2CONH_2$, K_2CO_3, KI, 2-butanone, Δ, 48 h, 53−98%; (f) $BH_3{\cdot}S(CH_3)_2$, diglyme, 90 °C, 16 h, 61−88%; (g) *N*-(2-hydroxyethyl)phthalimide, Ph_3P, DEAD, THF, Δ, 15 h, 50%; (h) $N_2H_4{\cdot}H_2O$, CH_3COOH, EtOH, Δ, 3 h, 33%.

synthesized compounds were inactive or poorly active at other 5-HT receptor subtypes (Table 2). In particular, unsubstituted compound **8** showed the best selectivity profile for the 5-HT_{1A}R.

The new identified high-affinity 5-HT_{1A}R ligands [$K_i \leq 25$ nM (Table 2)] were considered for functional characterization at the 5-HT_{1A}R (Table 3), in parallel with *in vitro* pharmacokinetic studies (Table 4).

Functional Activity at the 5-HT_{1A}R. The functional role of the new ligands at the 5-HT_{1A}R was characterized both *in vitro* and *in vivo*. The *in vitro* agonist action was studied by measuring the inhibition of forskolin-stimulated cyclic adenosine monophosphate (cAMP) formation in HeLa cells transfected with the human 5-HT_{1A}R (h5-HT_{1A}R). The *in vivo* test of 5-HT_{1A}R stimulation consisted of the hypothermic response in mice (sensitive to the selective 5-HT_{1A}R antagonist WAY-100635). Assayed compounds **8**, **16**, **19**, and **32** behaved as agonists in the cell line transfected with the h5-HT_{1A}R, with EC_{50} values for adenylyl cyclase inhibition in the range of 19−76 nM (Table 3). Notably, the most potent alkoxyphenyl derivatives, **16** and **19** (EC_{50} values of 23 and 19 nM, respectively), also exhibited the lowest minimal effective doses in the hypothermia assay (0.625 and 0.875 mg/kg, respectively).

***In Vitro* Pharmacokinetics.** High-affinity 5-HT_{1A}R ligands were also assessed for metabolic stability *in vitro* using rat and human liver microsomes (RLMs and HLMs, respectively), as a measure of first-pass metabolism. Test compounds were equilibrated at 37 °C with NADPH and $MgCl_2$ at concentrations of 1 and 5 μM; RLM and HLM preparations were added to initiate the reaction, and aliquots were withdrawn and quenched at different times (see the Experimental Section for details). The percent of parent compound remaining in the incubation mixture was determined by high-performance liquid chromatography and mass spectrometry (HPLC−MS) and plotted as a function of time. The half-life time ($t_{1/2}$) was determined from the slopes of the peak areas over time, which was then used to calculate the intrinsic clearance (CL_{int}).[41] From the results listed in Table 4, microsomal metabolism was found to be more favorable for HLMs than for RLMs. The data indicated that all assayed compounds exhibited high rates of metabolic degradation in rats, with $t_{1/2}$ values of 8−13 min and CL_{int} values of >100 mL/min/kg (Table 4). However, good rates were observed in human microsomes with $t_{1/2}$ values of 2−4 h and CL_{int} values of <5 mL/min/kg. Interestingly, the most potent compounds, **16** and **19** (K_i = 4.8 and 2.3 nM and EC_{50} = 23 and 19 nM, respectively), were also the most metabolically stable compounds, with good half-life and clearance values ($t_{1/2}$ = 3−4 h; CL_{int} = 2.6 and 3.5 mL/min/kg, respectively). In addition, the stability rate of compound **19** in mouse liver microsomes was 2-fold higher than that determined in rats [$t_{1/2}$ values of 29.5 and 13.1 min in mice and rats, respectively (Table 4)].

An *in vitro* fluorescence-based inhibition assay was conducted with cytochrome P450 2D6 (CYP2D6), one of the most impor-

dx.doi.org/10.1021/jm400766k | J. Med. Chem. 2013, 56, 7851−7861

Table 1. 5-HT$_{1A}$R Affinities of New Synthesized Compounds 4−35

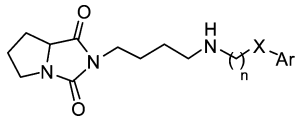

compd	n	X	Ar	$K_i \pm$ SEM (nM)[a,b]	compd	n	X	Ar	$K_i \pm$ SEM (nM)[a,b]
4	0	CH_2		>1000	**20**	2	O		37.43 ± 0.02
5	1	CH_2		868 ± 23	**21**	2	O		62 ± 6
6	2	CH_2		74 ± 5	**22**	2	O		52 ± 7
7	3	CH_2		138 ± 26	**23**	2	O		>1000
8	2	O		25.4 ± 0.8	**24**	2	O		>1000
9	2	O		16.8 ± 0.7	**25**	2	O		>1000
10	2	O		30 ± 5	**26**	2	O		>1000
11	2	O		742 ± 50	**27**	2	O		510 ± 125
12	2	O		38 ± 6	**28**	2	O		38.9 ± 0.6
13	2	O		26 ± 7	**29**	2	O		>1000
14	2	O		72 ± 5	**30**	2	O		45 ± 5
15	2	O		>1000	**31**	2	O		38 ± 10
16	2	O		4.8 ± 0.1	**32**	2	O		2.4 ± 0.6
17	2	O		34 ± 5	**33**	2	O		41 ± 6
18	2	O		>1000	**34**	2	O		27 ± 3
19	2	O		2.3 ± 0.1	**35**	2	O		44 ± 6
3									1.23 ± 0.09

[a]Values are means of two to four experiments performed in triplicate. [b]8-OH-DPAT was used as a reference compound (K_i = 1.02 ± 0.08 nM).

tant enzymes involved in drug metabolism, using human recombinant microsomal CYP2D6 enzyme, AMMC {3-[2-(*N*,*N*-diethyl-*N*-methylamino)ethyl]-7-methoxy-4-methylcoumarin} as a substrate, and quinidine as a control inhibitor. Table 4 shows the remaining activities of CYP2D6 after a 30 min incubation with assayed compounds at a concentration of 10 μM.

Selected compounds were also tested for interaction with human serum albumina (HSA), at a concentration of 5 μM, and the binding data are listed in Table 4. A correlation between

dx.doi.org/10.1021/jm400766k | J. Med. Chem. 2013, 56, 7851−7861

Table 2. Selectivity of High-Affinity 5-HT$_{1A}$R Ligands

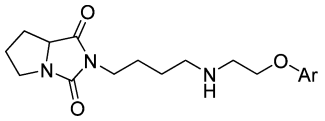

compd	Ar	$K_i \pm$ SEM (nM)[a]				
		5-HT$_{1A}$[b]	5-HT$_{2A}$[c]	5-HT$_3$[d]	5-HT$_4$[e]	5-HT$_7$[f]
8		25.4 ± 0.8	>1000	>1000	>1000	>1000
9		16.8 ± 0.7	366 ± 26	>1000	>1000	185 ± 32
10		30 ± 5	>1000	>1000	>1000	>1000
12		38 ± 6	260 ± 53	>1000	>1000	>1000
13		26 ± 7	>1000	>1000	>1000	101 ± 11
16		4.8 ± 0.1	267 ± 2	>1000	>1000	>1000
17		34 ± 5	>1000	>1000	>1000	>1000
19		2.3 ± 0.1	>1000	>1000	>1000	16.9 ± 0.9
20		37.43 ± 0.02	>1000	>1000	>1000	>1000
22		52 ± 7	514 ± 80	>1000	>1000	>1000
30		45 ± 5	310 ± 10	>1000	>1000	>1000
31		38 ± 10	49 ± 1	>1000	>1000	>1000
32		2.4 ± 0.6	41 ± 7	>1000	>1000	43 ± 4
33		41 ± 6	422 ± 35	>1000	>1000	>1000
34		27 ± 3	>1000	>1000	>1000	301 ± 47
35		44 ± 6	>1000	>1000	>1000	15 ± 2

[a]Values are means of two to four experiments performed in triplicate. [b]8-OH-DPAT was used as a reference compound (K_i = 1.02 ± 0.08 nM). [c]Ketanserin was used as a reference compound (K_i = 0.47 ± 0.04 nM). [d]Ondansetron was used as a reference compound (K_i = 0.77 ± 0.01 nM). [e]RS 39604 was used as a reference compound (K_i = 3.9 ± 0.2 nM). [f]5-CT was used as a reference compound (K_i = 1.8 ± 0.6 nM).

lipophilicity and protein binding can be observed, leading compounds **9** and **32** to exhibit the highest values of both clogP and HSA binding (clogP values of 2.33 and 2.48 and HSA binding of 55 and 60%, respectively). It is noteworthy that compounds **16** and **19**, showing the lowest HSA binding (25%), are the most potent agonists *in vivo* [minimal effective doses of 0.625 and 0.875 mg/kg, respectively (see Table 3)].

Altogether, these pharmacokinetic studies indicate that the new 5-HT$_{1A}$R agonists identified in this work display a promising pharmacokinetic profile *in vitro*.

Antinociceptive Activity in an *in Vivo* Model. According to the *in vitro* results (Tables 3 and 4), compounds **8**, **16**, **19**, and **32** endowed with high affinity, agonist potency for the 5-HT$_{1A}$R, and/or good pharmacokinetic properties were assessed for their potential analgesic activity *in vivo*. The new compounds were

dx.doi.org/10.1021/jm400766k | J. Med. Chem. 2013, 56, 7851−7861

Table 3. Functional Activities of High-Affinity 5-HT$_{1A}$R Ligands

compd	$K_i \pm$ SEM (nM)[a]	EC_{50} (nM)[b]	hypothermia (minimal effective dose, mg/kg)
8	25.4 ± 0.8	76	2.5
9	16.8 ± 0.7	1195 (PA)[c]	10
16	4.8 ± 0.1	23	0.625
19	2.3 ± 0.1	19	0.875
32	2.4 ± 0.6	45	10

[a]Values are means of two to four experiments performed in triplicate. [b]8-OH-DPAT was used as a reference compound (EC_{50} = 8 nM). [c]PA, partial agonist.

evaluated in the mouse formalin model of pain, which is an effective test for screening compounds for nociception.[42] Formalin injection induces a biphasic stereotypical nocifensive behavior. Nociceptive responses are divided into an early, short-lasting first phase (0−5 min), caused by formalin stimulus (phase I or early acute phase), followed by a quiescent period and then a second, prolonged phase (15−30 min) of persistent inflammatory pain (phase II or late chronic phase). Test substances and vehicle [0.2% hydroxypropyl methylcellulose (HPMC), 0.9% NaCl] were each administered by intraperitoneal injection (ip) or oral gavage (po) 15 or 30 min before subplantar injection of formalin (0.02 mL, 2% solution, ip), respectively. Hind paw licking time was recorded at 5 min intervals for 35 min following formalin injection. Statistical analysis using one-way analysis of variance (ANOVA) followed by Dunnett's test was applied for comparison between the test compound-treated and vehicle control groups (significance was considered at the $p < 0.05$ level). In these *in vivo* experiments, morphine, a substance widely used as a drug with pain-attenuating effect in humans, and gabapentin, a drug commonly used to relieve neuropathic pain, were also assayed for comparative purposes. As shown in Figure 1, at a dose of 3 mg/kg, the new 5-HT$_{1A}$R agonists reduced licking time in the second phase (15−30 min) of the nocifensive response to formalin in mice. The most efficacious compound, **19**, exhibited an antinociceptive effect also against the first phase (0−5 min) of formalin-induced nocifensive behavior (Figure 2A), when administered ip at a 30-fold smaller dose than gabapentin. Importantly, the selective 5-HT$_{1A}$R antagonist WAY-100635 completely blocked the analgesic activity of **19**, because no significant decrease in the duration of licks was observed after pretreatment with WAY-100635 (3 mg/kg, ip) 45 min before injection of formalin (Figure 2B). These results support the idea that the *in vivo* effect exhibited by compound **19** is mediated by the serotonin 5-HT$_{1A}$R. The specificity of agonist **19** was further confirmed by the assessment of binding affinity toward other nociception-related GPCRs.[43] Indeed, compound **19** was found to be inactive in α_2-adrenergic, cannabinoid CB_1 and CB_2, $GABA_B$, muscarinic M2 and M4, δ_2- and μ-opioid, and somatostatin (SST) receptors (see Table S1 of the Supporting Information).

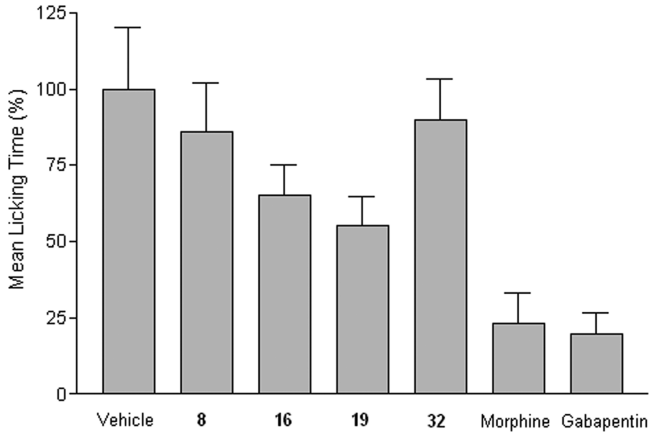

Figure 1. Effects of new 5-HT$_{1A}$R agonists on formalin-induced licking response in the late phase (15−30 min) of nociception. Vehicle (0.2% HPMC, 0.9% NaCl), test compounds (3 mg/kg), morphine (8 mg/kg), or gabapentin (100 mg/kg) was administered ip 15 min before subplantar injection of formalin (0.02 mL, 2% solution, ip). Licking time of the control group was 100%.

Moreover, orally administered **19** at a dose of 30 mg/kg was associated with a significant antinociceptive effect in both early and late phases (Figure 2C), and this analgesic activity was comparable to that of gabapentin (100 mg/kg, ip). No significant symptoms of toxicity were observed after the administration of tested compounds.

CONCLUSIONS

Herein we report the synthesis of new compounds **4**−**35**, based on two different openings (A and B) of the chromane ring present in the previously identified ligand **3** (Chart 2). The new analogues were assessed for binding affinity at the 5-HT$_{1A}$R and selectivity over other serotonin receptors (Tables 1 and 2). The newly characterized 5-HT$_{1A}$R agonists were also evaluated for their potential analgesic activity *in vivo* and pharmacokinetic properties *in vitro*. Compounds **8**, **16**, **19**, and **32** were identified as high-affinity and potent 5-HT$_{1A}$R agonists (Table 3) and afforded an ip antinociceptive effect against the second phase of the mouse intradermal formalin test (Figure 1). The antinociceptive effect of the most efficacious compound **19** (3 mg/kg, ip) was reversed by the selective 5-HT$_{1A}$R antagonist WAY-100635 (Figure 2), and its oral activity (30 mg/kg, po) was comparable to that of gabapentin, a drug commonly used to relieve neuropathic pain. Pharmacokinetic studies indicated that compound **19** displays a good metabolic stability in HLMs ($t_{1/2} \sim 3$ h and CL_{int} = 3.5 mL/min/kg at 5 μM) and a low level of protein binding (25% at 5 μM). Thus, the new 5-HT$_{1A}$R agonist identified in this work, **19** (n = 2, X = O, and Ar = 2-ethoxyphenyl), has been characterized as a high-affinity and potent 5-HT$_{1A}$R agonist (K_i = 2.3 nM; EC_{50} = 19 nM) endowed with oral

Table 4. *In Vitro* Pharmacokinetic Properties of New 5-HT$_{1A}$R Agonists

compd	RLM $t_{1/2}$ (min)	CL_{int} (mL/min/mg of protein)	HLM $t_{1/2}$ (min)	CL_{int} (mL/min/mg of protein)	CYP2D6 activity remaining (%)	human serum albumin (HSA) binding (%)	clogP[a]
8	10.0	140.3	151	4.1	24	38	1.31
9	10.7	131.2	137	4.6	13	55	2.33
16	9.7	144.7	237	2.6	48	25	1.04
19	13.1[b]	107.1	179	3.5	18	25	1.57
32	8.1	171.1	123	5.1	6	60	2.48

[a]Values were calculated using ChemBioDraw Ultra 11.0. [b]Stability was also determined in mouse liver microsomes: $t_{1/2}$ = 29.5 min.

dx.doi.org/10.1021/jm400766k | J. Med. Chem. 2013, 56, 7851−7861

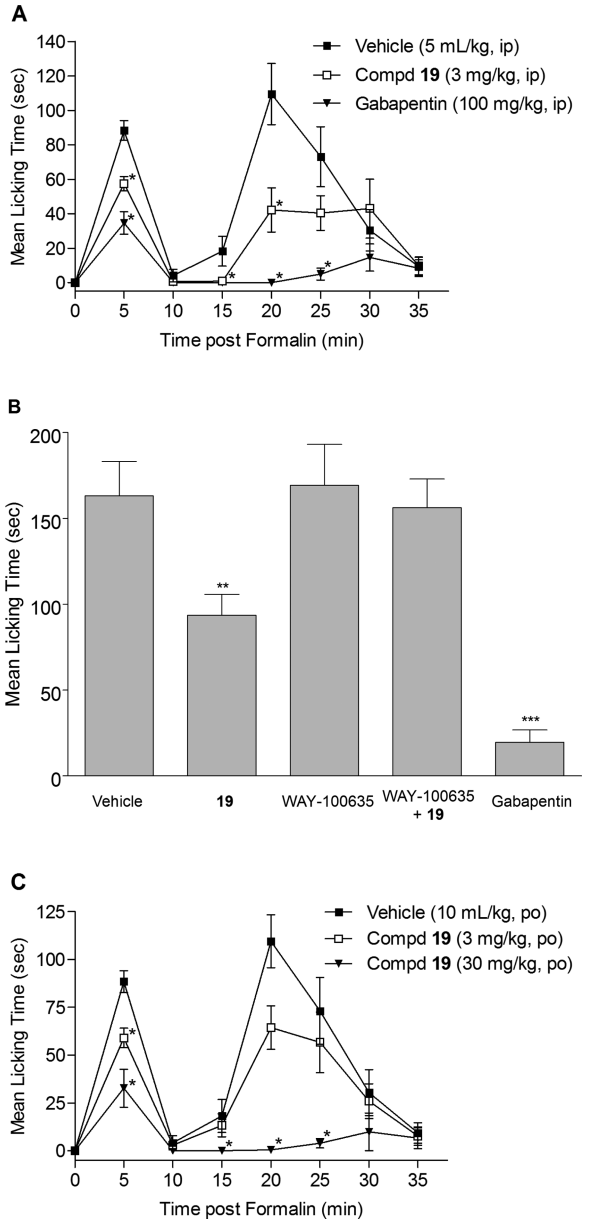

Figure 2. (A) Analgesic effect of compound **19** in the formalin test. Vehicle (0.2% HPMC, 0.9% NaCl), **19**, or gabapentin was administered ip 15 min before subplantar injection of formalin (0.02 mL, 2% solution, ip). (B) Effect of compound **19** (3 mg/kg, ip) during the late phase after pretreatment with WAY-100635 (3 mg/kg, ip) 45 min before formalin injection. (C) Analgesic effect of compound **19** in the formalin test when administered po 30 min before formalin injection. In all cases, hind paw licking time was recorded at 5 min intervals for 35 min following formalin injection. A one-way ANOVA followed by Dunnett's test was applied; one, two, or three asterisks indicate significant differences ($p < 0.05$, 0.01, or 0.001, respectively) vs vehicle control ($n = 10$).

analgesic activity *in vivo*. The results reported herein suggest the interest of compound **19** and represent a step toward identifying new therapeutics for the control of pain.

EXPERIMENTAL SECTION

Chemistry. Melting points (mp, uncorrected) were determined on a Stuart Scientific electrothermal apparatus. Infrared (IR) spectra were measured on a Shimadzu-8300 or Bruker Tensor 27 instrument equipped with a Specac ATR accessory with a transmission range of of 5200−650 cm^{-1}; frequencies (ν) are expressed in cm^{-1}. Nuclear magnetic resonance (NMR) spectra were recorded on a Bruker Avance 500 (^{1}H, 500 MHz; ^{13}C, 125 MHz), Bruker Avance 300-AM (^{1}H, 300 MHz; ^{13}C, 75 MHz), or Bruker 200-AC (^{1}H, 200 MHz; ^{13}C, 50 MHz) spectrometer at the Universidad Complutense de Madrid's NMR facilities. Chemical shifts (δ) are expressed in parts per million relative to internal tetramethylsilane; coupling constants (J) are in hertz. The following abbreviations are used to describe peak patterns when appropriate: s (singlet), d (doublet), t (triplet), q (quartet), qt (quintet), m (multiplet), and br (broad). Two-dimensional NMR experiments (HMQC and HMBC) of representative compounds were conducted to assign protons and carbons of the new structures. Elemental analyses (C, H, N) were obtained on a LECO CHNS-932 apparatus at the Universidad Complutense de Madrid's analysis services and were within 0.5% of the theoretical values, confirming a purity of at least 95% for all tested compounds. Analytical thin-layer chromatography (TLC) was conducted on Merck silica gel plates (Kieselgel 60 F-254) with detection by UV light (254 nm), a ninhydrin solution, or a 10% phosphomolybdic acid solution in ethanol. Flash chromatography was performed on a Varian 971-FP flash purification system using silica gel cartridges (Varian, particle size of 50 μm). Unless stated otherwise, starting materials, reagents, and solvents were purchased as high-grade commercial products from Sigma-Aldrich, Acros, Lancaster, Scharlab, or Panreac and were used without further purification. Anhydrous tetrahydrofuran (THF) and diethyl ether were distilled from sodium benzophenone ketyl and used immediately.

2-(4-Bromobutyl)tetrahydro-1*H*-pyrrolo[1,2-*c*]imidazole-1,3(2*H*)-dione (**36**)[32] and tetrahydro-1*H*-pyrrolo[1,2-*c*]imidazole-1,3(2*H*)-dione (**41**)[44] were synthesized according to described procedures, and their spectroscopic data correspond with those previously reported. Collected data for compounds **4**−**35** refer to free bases, and then hydrochloride salts were prepared prior to mp determination, elemental analyses, and biological assays. Spectroscopic data of all described compounds were consistent with the proposed structures. For final compounds **4**−**35**, we include the data of **8**, **9**, **16**, **19**, and **32**.

2-{4-[(2-Methoxybenzyl)amino]butyl}tetrahydro-1*H*-pyrrolo[1,2-*c*]imidazole-1,3(2*H*)-dione (4). Obtained from **36** and 2-methoxybenzylamine in 42% yield as an oil: chromatography in 1:9 hexane/ethyl acetate.

2-(4-{[2-(2-Methoxyphenyl)ethyl]amino}butyl)-tetrahydro-1*H*-pyrrolo[1,2-*c*]imidazole-1,3(2*H*)-dione (5). Obtained from **36** and 2-(2-methoxyphenyl)ethylamine in 30% yield as an oil: chromatography in 1:9 hexane/ethyl acetate.

2-(4-{[3-(2-Methoxyphenyl)propyl]amino}butyl)-tetrahydro-1*H*-pyrrolo[1,2-*c*]imidazole-1,3(2*H*)-dione (6). Obtained from **36** and 3-(2-methoxyphenyl)propylamine in 52% yield as an oil: chromatography in 95:5 toluene/methanol.

2-(4-{[4-(2-Methoxyphenyl)butyl]amino}butyl)-tetrahydro-1*H*-pyrrolo[1,2-*c*]imidazole-1,3(2*H*)-dione (7). Obtained from **36** and **37** in 30% yield as an oil: chromatography in 95:5 chloroform/methanol.

2-{4-[(2-Phenoxyethyl)amino]butyl}tetrahydro-1*H*-pyrrolo-[1,2-*c*]imidazole-1,3(2*H*)-dione (8). Obtained from **36** and **38a** in 54% yield as a solid: mp 154−155 °C (diethyl ether); chromatography in 9:1 dichloromethane/ethanol; IR ($CHCl_3$) ν 3315 (NH), 1770, 1709 (CO), 1599, 1587, 1497 (Ar); ^{1}H NMR ($CDCl_3$) δ 1.47−1.77 (m, 5H, $(CH_2)_2$, $^1/_2CH_{2cyc}$), 1.98−2.29 (m, 3H, CH_{2cyc}, $^1/_2CH_{2cyc}$), 2.70 (t, J = 6.8, 2H, C$\underline{H}_2$NH), 2.99 (t, J = 4.9, 2H, C$\underline{H}_2$NH), 3.23 (ddd, J = 11.2, 7.6, 5.2, 1H, $^1/_2CH_{2cyc}$), 3.49 (t, J = 7.3, 2H, NCH_2), 3.67 (dt, J = 11.2, 7.6, 1H, $^1/_2CH_{2cyc}$), 4.02−4.10 (m, 3H, CH, OCH_2), 6.87−6.98 (m, 3H, $3CH_{Ar}$), 7.23−7.32 (m, 2H, $2CH_{Ar}$); ^{13}C NMR ($CDCl_3$) δ 26.0, 27.1, 27.3, 27.7, 38.9, 45.7, 48.9, 49.4 ($8CH_2$), 63.4 (CH), 67.3 (CH_2), 114.7 (2CH), 121.0 (CH), 129.6 (2CH), 158.3 (C), 160.7, 174.0 (2CO). Anal. ($C_{18}H_{25}N_3O_3$·HCl) C, H, N.

2-(4-{[2-(2-Ethylphenoxy)ethyl]amino}butyl)tetrahydro-1*H*-pyrrolo[1,2-*c*]imidazole-1,3(2*H*)-dione (9). Obtained from **36** and **38b** in 69% yield as a solid: mp 183−185 °C (hexane); chromatography in 9:1 dichloromethane/ethanol; IR ($CHCl_3$) ν 3398 (NH), 1772, 1708 (CO), 1597, 1554, 1506 (Ar); ^{1}H NMR ($CDCl_3$) δ 1.19 (t, J = 7.4, 3H, CH_3), 1.59−1.74 (m, 5H, $(CH_2)_2$, $^1/_2CH_{2cyc}$), 1.97−2.09 (m, 2H, CH_{2cyc}), 2.17−2.28 (m, 1H, $^1/_2CH_{2cyc}$), 2.63 (q, J = 7.6, 2H, C$\underline{H}_2$$CH_3$),

dx.doi.org/10.1021/jm400766k | J. Med. Chem. 2013, 56, 7851−7861

2.80 (t, J = 7.1, 2H, C$\underline{H}_2$NH), 3.08 (t, J = 5.1, 2H, C$\underline{H}_2$NH), 3.17−3.29 (m, 1H, $^1/_2CH_{2cyc}$), 3.50 (t, J = 6.8, 2H, NCH_2), 3.61−3.75 (m, 1H, $^1/_2CH_{2cyc}$), 4.02−4.15 (m, 3H, OCH_2, CH), 6.82−6.94 (m, 2H, $2CH_{Ar}$), 7.11−7.17 (m, 2H, $2CH_{Ar}$); ^{13}C NMR ($CDCl_3$) δ 12.2 (CH_3), 23.2, 25.7, 26.6, 27.0, 27.5, 38.6, 45.5, 48.5, 48.9 ($9CH_2$), 63.3 (CH_2, CH), 111.3, 120.8, 126.8, 129.0 (4CH), 132.7, 156.3 (2C), 160.8, 167.4 (2CO). Anal. ($C_{20}H_{29}N_3O_3$·HCl) C, H, N.

2-(4-{[2-(3-Ethylphenoxy)ethyl]amino}butyl)tetrahydro-1*H*-pyrrolo[1,2-*c*]imidazole-1,3(2*H*)-dione (10). Obtained from **39** and **40a** in 43% yield as an oil: chromatography in ethyl acetate.

2-(4-{[2-(4-Ethylphenoxy)ethyl]amino}butyl)tetrahydro-1*H*-pyrrolo[1,2-*c*]imidazole-1,3(2*H*)-dione (11). Obtained from **39** and **40b** in 35% yield as an oil: chromatography in ethyl acetate.

2-(4-{[2-(2-Isopropylphenoxy)ethyl]amino}butyl)tetrahydro-1*H*-pyrrolo[1,2-*c*]imidazole-1,3(2*H*)-dione (12). Obtained from **39** and **40c** in 23% yield as a solid: mp 134−136 °C (diethyl ether); chromatography in ethyl acetate.

2-(4-{[2-(1,1′-Biphenyl-2-yloxy)ethyl]amino}butyl)-tetrahydro-1*H*-pyrrolo[1,2-*c*]imidazole-1,3(2*H*)-dione (13). Obtained from **39** and **40d** in 35% yield as an oil: chromatography in 9:1 ethyl acetate/ethanol.

2-(4-{[2-(1,1′-Biphenyl-3-yloxy)ethyl]amino}butyl)-tetrahydro-1*H*-pyrrolo[1,2-*c*]imidazole-1,3(2*H*)-dione (14). Obtained from **39** and **40e** in 32% yield as an oil: chromatography in 9:1 ethyl acetate/ethanol.

2-(4-{[2-(1,1′-Biphenyl-4-yloxy)ethyl]amino}butyl)-tetrahydro-1*H*-pyrrolo[1,2-*c*]imidazole-1,3(2*H*)-dione (15). Obtained from **39** and **40f** in 30% yield as an oil: chromatography in 9:1 ethyl acetate/ethanol.

2-(4-{[2-(2-Methoxyphenoxy)ethyl]amino}butyl)tetrahydro-1*H*-pyrrolo[1,2-*c*]imidazole-1,3(2*H*)-dione (16). Obtained from **36** and **38c** in 56% yield as a solid: mp 126−127 °C (diethyl ether); chromatography in 9:1 dichloromethane/ethanol; IR ($CHCl_3$) ν 3385 (NH), 1771, 1709 (CO), 1493, 1445 (Ar); ^{1}H NMR ($CDCl_3$) δ 1.63−1.71 (m, 5H, $(CH_2)_2$, $^1/_2CH_{2cyc}$), 1.99−2.29 (m, 3H, CH_{2cyc}, $^1/_2CH_{2cyc}$), 2.78 (t, J = 6.8, 2H, C$\underline{H}_2$NH), 3.01−3.10 (m, 2H, C$\underline{H}_2$NH), 3.21 (ddd, J = 11.2, 6.1, 5.6, 1H, $^1/_2CH_{2cyc}$), 3.57−3.80 (m, 3H, NCH_2, $^1/_2CH_{2cyc}$), 3.83 (s, 3H, OCH_3), 4.00−4.18 (m, 3H, OCH_2, CH), 6.87−6.90 (m, 4H, $4CH_{Ar}$); ^{13}C NMR ($CDCl_3$) δ 25.5, 25.6, 26.5, 27.4, 38.4, 45.4, 48.1, 48.6 ($8CH_2$), 63.2 (CH), 67.7 (CH_3), 71.0 (CH_2), 111.8, 120.9, 125.9, 129.7 (4CH), 130.5, 147.8 (2C), 160.6, 173.9 (2CO). Anal. ($C_{19}H_{27}N_3O_4$·HCl·$4H_2O$) C, H, N.

2-(4-{[2-(3-Methoxyphenoxy)ethyl]amino}butyl)tetrahydro-1*H*-pyrrolo[1,2-*c*]imidazole-1,3(2*H*)-dione (17). Obtained from **36** and **38d** in 35% yield as a solid: mp 124−126 °C (diethyl ether); chromatography in 9:1 dichloromethane/ethanol.

2-(4-{[2-(4-Methoxyphenoxy)ethyl]amino}butyl)tetrahydro-1*H*-pyrrolo[1,2-*c*]imidazole-1,3(2*H*)-dione (18). Obtained from **39** and **40g** in 32% yield as an oil: chromatography in 9:1 dichloromethane/ethanol.

2-(4-{[2-(2-Ethoxyphenoxy)ethyl]amino}butyl)tetrahydro-1*H*-pyrrolo[1,2-*c*]imidazole-1,3(2*H*)-dione (19). Obtained from **36** and **38e** in 30% yield as an oil: chromatography in ethyl acetate; IR ($CHCl_3$) ν 3422 (NH), 1773, 1707 (CO), 1593, 1541, 1505, 1445 (Ar); ^{1}H NMR ($CDCl_3$) δ 1.43 (t, J = 6.8, 3H, CH_3), 1.62−1.72 (m, 5H, $(CH_2)_2$, $^1/_2CH_{2cyc}$), 1.94−2.27 (m, 3H, CH_{2cyc}, $^1/_2CH_{2cyc}$), 2.78 (t, J = 6.6, 2H, C$\underline{H}_2$NH), 3.06 (t, J = 5.1, 2H, C$\underline{H}_2$NH), 3.22 (ddd, J = 11.2, 7.3, 5.1, 1H, $^1/_2CH_{2cyc}$), 3.44−3.72 (m, 3H, NCH_2, $^1/_2CH_{2cyc}$), 4.01−4.17 (m, 5H, OCH_2, CH, C$\underline{H}_2$CH$_3$), 6.87−6.92 (m, 4H, $4CH_{Ar}$); ^{13}C NMR ($CDCl_3$) δ 14.8 (CH_3), 25.6, 26.4, 26.8, 27.4, 38.5, 45.4, 48.3, 48.7 ($8CH_2$), 63.2 (CH), 64.3, 68.3 ($2CH_2$), 113.6, 115.1, 120.9, 121.8 (4CH), 148.3, 149.1 (2C), 160.7, 173.8 (2CO). Anal. ($C_{20}H_{29}N_3O_4$·HCl·$4H_2O$) C, H, N.

2-(4-{[2-(4-Fluoro-2-methoxyphenoxy)ethyl]amino}butyl)-tetrahydro-1*H*-pyrrolo[1,2-*c*]imidazole-1,3(2*H*)-dione (20). Obtained from **36** and **38f** in 24% yield as a solid: mp 114−116 °C (diethyl ether); chromatography in 95:5 dichloromethane/ethanol.

2-(4-{[2-(2-Bromophenoxy)ethyl]amino}butyl)tetrahydro-1*H*-pyrrolo[1,2-*c*]imidazole-1,3(2*H*)-dione (21). Obtained from **39** and **40h** in 48% yield as a solid: mp 98−99 °C (hexane); chromatography in ethyl acetate.

2-(4-{[2-(3-Bromophenoxy)ethyl]amino}butyl)tetrahydro-1*H*-pyrrolo[1,2-*c*]imidazole-1,3(2*H*)-dione (22). Obtained from **39** and **40i** in 42% yield as a solid: mp 140−143 °C (hexane); chromatography in ethyl acetate.

2-(4-{[2-(4-Bromophenoxy)ethyl]amino}butyl)tetrahydro-1*H*-pyrrolo[1,2-*c*]imidazole-1,3(2*H*)-dione (23). Obtained from **39** and **40j** in 46% yield as a solid: mp 166−167 °C (hexane); chromatography in ethyl acetate.

2-(2-{[4-(1,3-Dioxotetrahydro-1*H*-pyrrolo[1,2-*c*]imidazol-2(3*H*)-yl)butyl]amino}ethoxy)benzonitrile (24). Obtained from **39** and **40k** in 42% yield as an oil: chromatography in ethyl acetate.

3-(2-{[4-(1,3-Dioxotetrahydro-1*H*-pyrrolo[1,2-*c*]imidazol-2(3*H*)-yl)butyl]amino}ethoxy)benzonitrile (25). Obtained from **39** and **40l** in 38% yield as an oil: chromatography in ethyl acetate.

4-(2-{[4-(1,3-Dioxotetrahydro-1*H*-pyrrolo[1,2-*c*]imidazol-2(3*H*)-yl)butyl]amino}ethoxy)benzonitrile (26). Obtained from **39** and **40m** in 43% yield as an oil: chromatography in ethyl acetate.

2-[4-({2-[2-(Trifluoromethyl)phenoxy]ethyl}amino)butyl]-tetrahydro-1*H*-pyrrolo[1,2-*c*]-imidazole-1,3(2*H*)-dione (27). Obtained from **39** and **40n** in 30% yield as an oil: chromatography in 9:1 ethyl acetate/ethanol.

2-[4-({2-[3-(Trifluoromethyl)phenoxy]ethyl}amino)butyl]-tetrahydro-1*H*-pyrrolo[1,2-*c*]imidazole-1,3(2*H*)-dione (28). Obtained from **39** and **40o** in 30% yield as an oil: chromatography in 9:1 ethyl acetate/ethanol.

2-[4-({2-[4-(Trifluoromethyl)phenoxy]ethyl}amino)butyl]-tetrahydro-1*H*-pyrrolo[1,2-*c*]imidazole-1,3(2*H*)-dione (29). Obtained from **39** and **40p** in 30% yield as an oil: chromatography in 9:1 ethyl acetate/ethanol.

2-(4-{[2-(2,3-Dimethylphenoxy)ethyl]amino}butyl)-tetrahydro-1*H*-pyrrolo[1,2-*c*]imidazole-1,3(2*H*)-dione (30). Obtained from **39** and **40q** in 30% yield as an oil: chromatography in 9:1 ethyl acetate/ethanol.

2-(4-{[2-(5,6,7,8-Tetrahydronaphthalen-1-yloxy)ethyl]-amino}butyl)tetrahydro-1*H*-pyrrolo[1,2-*c*]imidazole-1,3(2*H*)-dione (31). Obtained from **39** and **40r** in 32% yield as an oil: chromatography in 9:1 ethyl acetate/ethanol.

2-(4-{[2-(1-Naphthyloxy)ethyl]amino}butyl)tetrahydro-1*H*-pyrrolo[1,2-*c*]imidazole-1,3(2*H*)-dione (32). Obtained from **36** and **38g** in 48% yield as a solid: mp 163−164 °C (ethyl acetate); chromatography in 9:1 dichloromethane/ethanol; IR ($CHCl_3$) ν 3354 (NH), 1771, 1707 (CO), 1582, 1508 (Ar); ^{1}H NMR ($CDCl_3$) δ 1.58−1.77 (m, 5H, $(CH_2)_2$, $^1/_2CH_{2cyc}$), 1.93−2.30 (m, 3H, CH_{2cyc}, $^1/_2CH_{2cyc}$), 2.86 (t, J = 7.1, 2H, C$\underline{H}_2$NH), 3.15−3.27 (m, 3H, C$\underline{H}_2$NH, $^1/_2CH_{2cyc}$), 3.49 (t, J = 6.8, 2H, NCH_2), 3.60−3.73 (m, 1H, $^1/_2CH_{2cyc}$), 4.05 (dd, J = 9.0, 7.3, 1H, CH), 4.30 (t, J = 4.9, 2H, OCH_2), 6.80 (dd, J = 8.5, 1.2, 1H, CH_{Ar}), 7.31−7.53 (m, 4H, $4CH_{Ar}$), 7.75−7.83 (m, 1H, CH_{Ar}), 8.22−8.28 (m, 1H, CH_{Ar}); ^{13}C NMR ($CDCl_3$) δ 25.7, 26.3, 27.0, 27.5, 38.5, 45.5, 48.3, 48.8 ($8CH_2$), 63.3 (CH), 66.7 (CH_2), 104.9, 120.6, 121.9, 125.3 (4CH), 125.5 (C), 125.8, 126.4, 127.5 (3CH), 134.5, 154.3 (2C), 160.8, 174.0 (2CO). Anal. ($C_{22}H_{27}N_3O_3$·HCl) C, H, N.

2-(4-{[2-(2-Naphthyloxy)ethyl]amino}butyl)tetrahydro-1*H*-pyrrolo[1,2-*c*]imidazole-1,3(2*H*)-dione (33). Obtained from **39** and **40s** in 26% yield as an oil: chromatography in ethyl acetate to 9:1 ethyl acetate/ethanol.

2-[4-({2-[(4-Methoxy-1-naphthyl)oxy]ethyl}amino)butyl]-tetrahydro-1*H*-pyrrolo[1,2-*c*]-imidazole-1,3(2*H*)-dione (34). Obtained from **39** and **40t** in 21% yield as an oil: chromatography in ethyl acetate to 9:1 ethyl acetate/ethanol.

2-(4-{[2-(8-Quinolinyloxy)ethyl]amino}butyl)tetrahydro-1*H*-pyrrolo[1,2-*c*]imidazole-1,3(2*H*)-dione (35). Obtained from **36** and **38h** in 38% yield as a solid: mp 189−191 °C; chromatography in 95:5 to 8:2 dichloromethane/methanol.

Stability Assays in Rat and Human Liver Microsomes. Compounds were incubated at 37 °C and a final concentration of 1 or 5 μM in PBS together with a solution of NADPH in PBS (final concentration of 2 mM) and a solution of $MgCl_2$ in PBS (final concentration of 5 mM). Metabolic reactions were initiated by the addition of a suspension of RLMs (male Sprague-Dawley rats pooled, Sigma-Aldrich) or HLMs (male human pooled, Sigma-Aldrich), respectively, at a final protein concentration of 1 mg/mL. The solutions were shaken in a vortex and

kept in a water bath open to the air at 37 °C. Aliquots of 100 μL were quenched at time zero and at seven points ranging to 1 h (RLM) or 2 h (HLM) when mixtures were poured into 100 μL of ice-cold acetonitrile. Quenched samples were centrifuged at 10000*g* for 5 min, and the supernatants were filtered through a polytetrafluoroethylene (PTFE) membrane syringe filter (pore size of 0.2 μm, Albet Labscience).

The relative loss of parent compound over the course of the incubation was monitored by HPLC−MS using an Agilent 1200LC-MSD VL instrument. HPLC separation was achieved with an Agilent Eclipse XDB-C18 column (5 μm, 4.6 mm × 150 mm) together with a guard column (5 μm, 4.6 mm × 12.5 mm). The gradient elution mobile phases consisted of A (95:5 water/methanol) and B (95:5 methanol/water) with 0.1% formic acid and 0.1% NH_4OH as solvent modifiers. MS analysis was performed with an electrospray ionization (ESI) source. The capillary voltage was set to 3.0 kV, and the fragmentor voltage was set at 70 eV. The drying gas temperature was 350 °C; the drying gas flow rate was 10 L/min, and the nebulizer pressure was 20 psi. HPLC−MS measurements were made by selected ion monitoring (SIM).

Concentrations were quantified by measuring the area under the peak ($M + H^+$) and converted to the percentage of compound remaining, using the time zero peak area value as 100%. The natural logarithm of the percentage remaining versus time data for each compound was fit to linear regression, and the slope was used to calculate the degradation half-life. The latter was then used to calculate the intrinsic plasma clearance (CL_{int}) according to the methods of Obach.[41]

HSA Binding Assay. The assessment of compounds binding to HSA was performed by incubating a fixed concentration of the compound with different concentrations of immobilized HSA, using the TRANSIL^{XL} HSA Binding Kit (TMP-0210-2096, Sovicell). An eight-well unit of the TRANSIL assay plate was used for each compound; six wells contain increasing concentrations of HSA immobilized on silica beads suspended in PBS at pH 7.4, and two wells contain buffer only and serve as references to account for nonspecific binding.

The TRANSIL assay plate was thawed for 3 h at room temperature and centrifuged at 750*g* for 5 s. Then, 15 μL of an 80 μM stock solution of the compound in PBS (for a final concentration of 5 μM) was added to each well of the eight-well unit, and the plate was incubated on a plate shaker at 1000 rpm for 12 min at room temperature. After this time, the plate was centrifuged at 750*g* for 10 min, and 50 μL of the supernatants was transferred for analytical quantification by HPLC−MS.

The binding percentage was calculated from the remaining free compound concentration in the supernatant of each well, using the spreadsheet and algorithms supplied with the kit.

Fluorescence-Based CYP2D6 Inhibition Assay. Effects on CYP2D6 activity were determined at Suven Life Sciences (Banjara Hills, Hyderabad, India). Briefly, after incubation for 30 min of the test compound (10 μM) in microsomes containing human recombinant CYP2D6 (BD Biosciences, 0.015 μM), the conversion of AMMC (3 μM) to 3-[2-(*N*,*N*-diethylamino)ethyl]-7-hydroxy-4 methylcoumarin (AHMC) was measured, using a Spectra Max Gemini EM spectrofluorometer with a 390 nm excitation filter and a 460 nm emission filter. CYP2D6 activity is expressed as the percentage of the maximal effect obtained with substrate and no inhibitor. Quinidine was used as a control, and the IC_{50} value was found to be 0.002 μM, which is consistent with the value reported in the kit.

Formalin Test.[45] Male CD-1 (*Crl.*)-derived mice weighing 24 ± 2 g were provided by BioLasco Taiwan (Charles River Laboratories Technology Licensee). Space allocation for 10 animals was 47 cm × 18 cm × 13 cm. All animals were maintained in a controlled temperature (23−24 °C) and humidity (60−70%) environment with 12 h light/dark cycles for at least 1 week in MDS Pharma Services Taiwan Laboratory prior to use. Free access to standard lab chow for mice [MF-18 (Oriental Yeast Co., Ltd.)] and RO water was granted. All aspects of the assay, including housing, experimentation, and disposal of animals, were performed in general accordance with the Guide for the Care and Use of Laboratory Animals. Gabapentin was from Pfizer, and HMPC was from Sigma. The following equipment was used for the assay: animal cage (Allentown), beaker (1000 mL, Kimax), brown flask (50 mL), glass syringe (1 mL, Top Corp.), hypodermic needle (25 gauge × 1 in.) (TOP Corp.), mouse scale (Z-40, Taconic), needle for formalin injection (TOP Corp.), needle for oral administration (Natsume), and stop watch (World Leader).

Test substances and vehicle were each administered to groups of 10 mice by ip injection (5 mL/kg) or po gavage (10 mL/kg) for 15 or 30 min, respectively, before subplantar injection of formalin (0.02 mL, 2% solution). In the vehicle group, half of the animals were treated with 0.2% HPMC and 0.9% NaCl via ip and the other half via po. Reduction of the formalin-induced hind paw licking time was recorded at 5 min intervals during the following 0−35 min after formalin injection. To study the receptor specificity of compound **19**, WAY-100635 was administered ip 45 min before the injection of formalin. Statistical analysis was performed by using a one-way ANOVA followed by Dunnett's test to compare the test compound-treated and vehicle control groups. Significance is considered at the $p < 0.05$ level.

■ ASSOCIATED CONTENT

Ⓢ Supporting Information

Binding affinity data of **19** toward other nociception-related GPCRs, synthesis of compounds **4**−**35**, **37**, **38a**−**h**, **39**, **40a**−**t**, **42**, and **43a**−**g**, spectral characterization data of compounds **4**−**7**, **10**−**15**, **17**, **18**, **20**−**31**, and **33**−**35**, combustion analysis data of final compounds **4**−**35**, binding assays at 5-HT_{1A}, 5-HT_{2A}, 5-HT_3, 5-HT_4, and 5-HT_7 receptors, rectal temperatures, and cAMP formation in HeLa cells transfected with the h5-HT_{1A}R. This material is available free of charge via the Internet at http://pubs.acs.org.

■ AUTHOR INFORMATION

Corresponding Authors

*Phone: 34-91-3944239. Fax: 34-91-3944103. E-mail: mluzlr@quim.ucm.es.

*Phone: 34-91-3945156. Fax: 34-91-3944103. E-mail: bellinda.benhamu@quim.ucm.es.

Present Addresses

‖M.V.: Department of Chemistry, Yale University, West Haven, CT 06516.

⊥I.M.: Clarke, Modet & C°, 28001 Madrid, Spain.

Author Contributions

M.V. and I.M. contributed equally to this work.

Notes

The authors declare no competing financial interest.

■ ACKNOWLEDGMENTS

This work was supported by grants from MINECO (SAF2010-22198-C02-01), CAM (S2011/BMD2353), and UCB Pharma GmbH. M.V. is grateful to UCB Pharma GmbH for a predoctoral fellowship. We thank the NMR Core Facilities from Universidad Complutense de Madrid.

■ ABBREVIATIONS

AHMC, 3-[2-(*N*,*N*-diethylamino)ethyl]-7-hydroxy-4-methylcoumarin; AMMC, 3-[2-(*N*,*N*-diethyl-*N*-methylamino)ethyl]-7-methoxy-4-methylcoumarin; CL_{int}, intrinsic clearance; DMEM, Dulbecco's modified Eagle's medium; FCS, fetal calf serum; h5-HT_{1A}R, human 5-HT_{1A} receptor; HLMs, human liver microsomes; HPMC, hydroxypropyl methylcellulose; PTFE, polytetrafluoroethylene; RLMs, rat liver microsomes

■ REFERENCES

(1) Nichols, D. E.; Nichols, C. D. Serotonin receptors. *Chem. Rev.* **2008**, *108*, 1614−1641.

(2) Fargin, A.; Raymond, J. R.; Lohse, M. J.; Kobilka, B. K.; Caron, M. G.; Lefkowitz, R. J. The genomic clone G-21 which resembles a β-

adrenergic-receptor sequence encodes the 5-HT_{1A} receptor. *Nature* **1988**, *335*, 358−360.
(3) Lopez-Rodriguez, M. L.; Ayala, D.; Benhamu, B.; Morcillo, M. J.; Viso, A. Arylpiperazine derivatives acting at 5-HT_{1A} receptors. *Curr. Med. Chem.* **2002**, *9*, 443−469.
(4) Caliendo, G.; Santagada, V.; Perissutti, E.; Fiorino, F. Derivatives as 5-HT(1A) receptor ligands: Past and present. *Curr. Med. Chem.* **2005**, *12*, 1721−1753.
(5) Lacivita, E.; Leopoldo, M.; Berardi, F.; Perrone, R. 5-HT_{1A} receptor, an old target for new therapeutic agents. *Curr. Top. Med. Chem.* **2008**, *8*, 1024−1034.
(6) Ohno, Y. Therapeutic role of 5-HT_{1A} receptors in the treatment of schizophrenia and Parkinson's disease. *CNS Neurosci. Ther.* **2011**, *17*, 58−65.
(7) Lacivita, E.; Di Pilato, P.; De Giorgio, P.; Colabufo, N. A.; Berardi, F.; Perrone, R.; Leopoldo, M. The therapeutic potential of 5-HT_{1A} receptors: A patent review. *Expert Opin. Ther. Pat.* **2012**, *22*, 887−902.
(8) Schreiber, R.; Devry, J. 5-HT_{1A} receptor ligands in animal-models of anxiety, impulsivity and depression: Multiple mechanisms of action. *Prog. Neuro-Psychopharmacol. Biol. Psychiatry* **1993**, *17*, 87−104.
(9) Blier, P.; Ward, N. M. Is there a role for 5-HT_{1A} agonists in the treatment of depression? *Biol. Psychiatry* **2003**, *53*, 193−203.
(10) Savitz, J.; Lucki, I.; Drevets, W. C. 5-HT_{1A} receptor function in major depressive disorder. *Prog. Neurobiol.* **2009**, *88*, 17−31.
(11) Bantick, R. A.; Deakin, J. F. W.; Grasby, P. M. The 5-HT_{1A} receptor in schizophrenia: A promising target for novel atypical neuroleptics? *J. Psychopharmacol.* **2001**, *15*, 37−46.
(12) Caicoya, A. G.; Beneytez, M. L.; Delgado, M.; Manzanares, J.; Lopez-Rodriguez, M. L.; Benhamu, B.; Morcillo, M. J.; Pozo, M. A.; Rubia, F. J.; Fuentes, J. A. Biochemical, electrophysiological and neurohormonal studies with B-20991, a selective 5-HT_{1A} receptor agonist. *Pharmacology* **2001**, *62*, 234−242.
(13) Delgado, M.; Caicoya, A. G.; Greciano, V.; Benhamu, B.; Lopez-Rodriguez, M. L.; Fernandez-Alfonso, M. S.; Pozo, M. A.; Manzanares, J.; Fuentes, J. A. Anxiolytic-like effect of a serotonergic ligand with high affinity for 5-HT_{1A}, 5-HT_{2A} and 5-HT_3 receptors. *Eur. J. Pharmacol.* **2005**, *511*, 9−19.
(14) McCreary, A. C.; Jones, C. A. Antipsychotic medication: The potential role of 5-HT_{1A} receptor agonism. *Curr. Pharm. Des.* **2010**, *16*, 516−521.
(15) Liu, Z.; Zhang, H.; Ye, N.; Zhang, J.; Wu, Q.; Sun, P.; Li, L.; Zhen, X.; Zhang, A. Synthesis of dihydrofuroaporphine derivatives: Identification of a potent and selective serotonin 5-HT_{1A} receptor agonist. *J. Med. Chem.* **2010**, *53*, 1319−1328.
(16) Madhavan, L.; Freed, W. J.; Anantharam, V.; Kanthasamy, A. G. 5-Hydroxytryptamine 1A receptor activation protects against *N*-methyl-D-aspartate-induced apoptotic cell death in striatal and mesencephalic cultures. *J. Pharmacol. Exp. Ther.* **2003**, *304*, 913−923.
(17) Berends, A. C.; Luiten, P. G.; Nyakas, C. A review of the neuroprotective properties of the 5-HT_{1A} receptor agonist repinotan HCl (BAYx3702) in ischemic stroke. *CNS Drug Rev.* **2005**, *11*, 379−402.
(18) Chang, C. P.; Chen, S. H.; Lin, M. T. Ipsapirone and ketanserin protects against circulatory shock, intracranial hypertension, and cerebral ischemia during heatstroke. *Shock* **2005**, *24*, 336−340.
(19) Iannuzzi, N. P.; Liebeskind, D. S.; Jacoby, M.; Arima, K.; Shimizu, K.; Asubio, D.; Zimmerman, T. R. Piclozotan (SUN N4057), a novel 5-HT_{1A} receptor agonist, is well tolerated in patients with acute stroke. *Stroke* **2006**, *37*, 655−655.
(20) Kamei, K.; Maeda, N.; Nomura, K.; Shibata, M.; Katsuragi-Ogino, R.; Koyama, M.; Nakajima, M.; Inoue, T.; Ohno, T.; Tatsuoka, T. Synthesis, SAR studies, and evaluation of 1,4-benzoxazepine derivatives as selective 5-HT_{1A} receptor agonists with neuroprotective effect: Discovery of piclozotan. *Bioorg. Med. Chem.* **2006**, *14*, 1978−1992.
(21) Teal, P.; Davis, S.; Hacke, W.; Kaste, M.; Lyden, P. D.; Fierus, M. A randomized, double-blind, placebo-controlled trial to evaluate the efficacy, safety, tolerability, and pharmacokinetic/pharmacodynamic effects of a targeted exposure of intravenous repinotan in patients with acute ischemic stroke modified randomized exposure controlled trial. *Stroke* **2009**, *40*, 3518−3525.
(22) Marco, I.; Valhondo, M.; Martin-Fontecha, M.; Vazquez-Villa, H.; Del Rio, J.; Planas, A.; Sagredo, O.; Ramos, J. A.; Torrecillas, I. R.; Pardo, L.; Frechilla, D.; Benhamu, B.; Lopez-Rodriguez, M. L. New serotonin 5-HT_{1A} receptor agonists with neuroprotective effect against ischemic cell damage. *J. Med. Chem.* **2011**, *54*, 7986−7999.
(23) Bara-Jimenez, W.; Bibbiani, F.; Morris, M. J.; Dimitrova, T.; Sherzai, A.; Mouradian, M. M.; Chase, T. N. Effects of serotonin 5-HT_{1A} agonist in advanced Parkinson's disease. *Mov. Disord.* **2005**, *20*, 932−936.
(24) Fox, S. H.; Chuang, R.; Brotchie, J. M. Serotonin and Parkinson's disease: On movement, mood, and madness. *Mov. Disord.* **2009**, *24*, 1255−1266.
(25) Mico, J. A.; Berrocoso, E.; Ortega-Alvaro, A.; Gibert-Rahola, J.; Rojas-Corrales, M. O. The role of 5-HT_{1A} receptors in research strategy for extensive pain treatment. *Curr. Top. Med. Chem.* **2006**, *6*, 1997−2003.
(26) Colpaert, F. C.; Tarayre, J. P.; Koek, W.; Pauwels, P. J.; Bardin, L.; Xu, X. J.; Wiesenfeld-Hallin, Z.; Cosi, C.; Carilla-Durand, E.; Assie, M. B.; Vacher, B. Large-amplitude 5-HT_{1A} receptor activation: A new mechanism of profound, central analgesia. *Neuropharmacology* **2002**, *43*, 945−958.
(27) Colpaert, F. C. 5-HT_{1A} receptor activation: New molecular and neuroadaptive mechanisms of pain relief. *Curr. Opin. Invest. Drugs* **2006**, *7*, 40−47.
(28) Bardin, L.; Tarayre, J. P.; Malfetes, N.; Koek, W.; Colpaert, F. C. Profound, non-opioid analgesia produced by the high-efficacy 5-HT_{1A} agonist F 13640 in the formalin model of tonic nociceptive pain. *Pharmacology* **2003**, *67*, 182−194.
(29) Bang-Andersen, B.; Faldt, A.; Moerk, A.; Lopez De Diego, H.; Holm, R.; Stensboel, T. B.; Ringgaard, L. M.; Mealy, M. J.; Rock, M. H.; Brodersen, J.; Joergensen, M.; Moore, N. PCT/DK2007/050075, WO 2007/144005 A1, 2007.
(30) Moore, N.; Stensboel, T. B. PCT/DK2008/050063, WO 2008/113359 A2, 2008.
(31) https://www.clinicaltrialsregister.eu/ctr-search/search?query=F13640+and+pain.
(32) Lopez-Rodriguez, M. L.; Rosado, M. L.; Benhamu, B.; Morcillo, M. J.; Sanz, A. M.; Orensanz, L.; Beneitez, M. E.; Fuentes, J. A.; Manzanares, J. Synthesis and structure-activity relationships of a new model of arylpiperazines. 1. 2-[[4-(*o*-Methoxyphenyl)piperazin-1-yl]-methyl]-1,3-dioxoperhydroimidazo[1,5-*a*]pyridine: A selective 5-HT_{1A} receptor agonist. *J. Med. Chem.* **1996**, *39*, 4439−4450.
(33) Lopez-Rodriguez, M. L.; Morcillo, M. J.; Fernández, E.; Porras, E.; Murcia, M.; Sanz, A. M.; Orensanz, L. Synthesis and structure-activity relationships of a new model of arylpiperazines. 3. 2-[*ω*-(4-Arylpiperazin-1-yl)alkyl]perhydropyrrolo[1,2-*c*]imidazoles and -perhydroimidazo[1,5-a]pyridines: Study of the influence of the terminal amide fragment on 5-HT_{1A} affinity/selectivity. *J. Med. Chem.* **1997**, *40*, 2653−2656.
(34) Lopez-Rodriguez, M. L.; Morcillo, M. J.; Fernandez, E.; Porras, E.; Orensanz, L.; Beneytez, M. E.; Manzanares, J.; Fuentes, J. A. Synthesis and structure-activity relationships of a new model of arylpiperazines. 5. Study of the physicochemical influence of the pharmacophore on 5-HT_{1A}/α_1-adrenergic receptor affinity: Synthesis of a new derivative with mixed 5-HT_{1A}/D_2 antagonist properties. *J. Med. Chem.* **2001**, *44*, 186−197.
(35) Lopez-Rodriguez, M. L.; Morcillo, M. J.; Fernandez, E.; Rosado, M. L.; Pardo, L.; Schaper, K. J. Synthesis and structure-activity relationships of a new model of arylpiperazines. 6. Study of the 5-HT_{1A}/α_1-adrenergic receptor affinity by classical Hansch analysis, artificial neural networks, and computational simulation of ligand recognition. *J. Med. Chem.* **2001**, *44*, 198−207.
(36) Lopez-Rodriguez, M. L.; Ayala, D.; Viso, A.; Benhamu, B.; de la Pradilla, R. F.; Zarza, F.; Ramos, J. A. Synthesis and structure-activity relationships of a new model of arylpiperazines. Part 7: Study of the influence of lipophilic factors at the terminal amide fragment on 5-HT_{1A} affinity/selectivity. *Bioorg. Med. Chem.* **2004**, *12*, 1551−1557.
(37) Lopez-Rodriguez, M. L.; Morcillo, M. J.; Fernandez, E.; Benhamu, B.; Tejada, I.; Ayala, D.; Viso, A.; Campillo, M.; Pardo, L.; Delgado, M.;

Manzanares, J.; Fuentes, J. A. Synthesis and structure-activity relationships of a new model of arylpiperazines. 8. Computational simulation of ligand-receptor interaction of 5-HT_{1A}R agonists with selectivity over α_1-adrenoceptors. *J. Med. Chem.* **2005**, *48*, 2548−2558.
(38) Lopez-Rodriguez, M. L.; Benhamu, B.; del Rio, J.; Frechilla, D.; Marco, I. PCT/EP2005/000840, WO 2005/075480 A1, 2005.
(39) Stohr, T.; Lopez-Rodriguez, M. L.; Benhamu, B. PCT/IB2007/002194, WO2008/015538 A2, 2008.
(40) Cheng, Y.; Prusoff, W. H. Relationship between the inhibition constant (Ki) and the concentration of inhibitor which causes 50% inhibition (I_{50}) of an enzymatic reaction. *Biochem. Pharmacol.* **1973**, *22*, 3099−3108.
(41) Obach, R. S.; Baxter, J. G.; Liston, T. E.; Silber, B. M.; Jones, B. C.; MacIntyre, F.; Rance, D. J.; Wastall, P. The prediction of human pharmacokinetic parameters from preclinical and in vitro metabolism data. *J. Pharmacol. Exp. Ther.* **1997**, *283*, 46−58.
(42) Vissers, K. C. P.; Geenen, F.; Biermans, R.; Meert, T. F. Pharmacological correlation between the formalin test and the neuropathic pain behavior in different species with chronic constriction injury. *Pharmacol., Biochem. Behav.* **2006**, *84*, 479−486.
(43) Pan, H.-L.; Wu, Z.-Z.; Zhou, H.-Y.; Chen, S.-R.; Zhang, H.-M.; Li, D.-P. Modulation of pain transmission by G-protein-coupled receptors. *Pharmacol. Ther.* **2008**, *117*, 141−161.
(44) Dakin, H. D. Amino acids of gelatin. *J. Biol. Chem.* **1920**, *44*, 499−529.
(45) Hunskaar, S.; Fasmer, O. B.; Hole, K. Formalin test in mice, a useful technique for evaluating mild analgesics. *J. Neurosci. Methods* **1985**, *14*, 69−76.